

# Artificial intelligence for the detection of glaucoma with SD-OCT images: a systematic review and Meta-analysis

Nan-Nan Shi<sup>1,2</sup>, Jing Li<sup>1,2</sup>, Guang-Hui Liu<sup>1,2</sup>, Ming-Fang Cao<sup>1,2</sup>

<sup>1</sup>Department of Ophthalmology, Affiliated People's Hospital (Fujian Provincial People's Hospital), Fujian University of Traditional Chinese Medicine, Fuzhou 350004, Fujian Province, China

<sup>2</sup>Eye Institute of Integrated Chinese and Western Medicine, Fujian University of Traditional Chinese Medicine, Fuzhou 350004, Fujian Province, China

**Correspondence to:** Ming-Fang Cao and Guang-Hui Liu. Department of Ophthalmology, Affiliated People's Hospital (Fujian Provincial People's Hospital), Fujian University of Traditional Chinese Medicine, 602 817 Middle Road, Taijiang District, Fuzhou 350004, Fujian Province, China. farrahcao@126.com; latiny@gmail.com

Received: 2023-08-16 Accepted: 2023-12-18

## Abstract

• **AIM:** To quantify the performance of artificial intelligence (AI) in detecting glaucoma with spectral-domain optical coherence tomography (SD-OCT) images.

• **METHODS:** Electronic databases including PubMed, Embase, Scopus, ScienceDirect, ProQuest and Cochrane Library were searched before May 31, 2023 which adopted AI for glaucoma detection with SD-OCT images. All pieces of the literature were screened and extracted by two investigators. Meta-analysis, Meta-regression, subgroup, and publication of bias were conducted by Stata16.0. The risk of bias assessment was performed in Revman5.4 using the QUADAS-2 tool.

• **RESULTS:** Twenty studies and 51 models were selected for systematic review and Meta-analysis. The pooled sensitivity and specificity were 0.91 (95%CI: 0.86–0.94,  $I^2=94.67\%$ ), 0.90 (95%CI: 0.87–0.92,  $I^2=89.24\%$ ). The pooled positive likelihood ratio (PLR) and negative likelihood ratio (NLR) were 8.79 (95%CI: 6.93–11.15,  $I^2=89.31\%$ ) and 0.11 (95%CI: 0.07–0.16,  $I^2=95.25\%$ ). The pooled diagnostic odds ratio (DOR) and area under curve (AUC) were 83.58 (95%CI: 47.15–148.15,  $I^2=100\%$ ) and 0.95 (95%CI: 0.93–0.97). There was no threshold effect (Spearman correlation coefficient=0.22,  $P>0.05$ ).

• **CONCLUSION:** There is a high accuracy for the detection of glaucoma with AI with SD-OCT images. The

application of AI-based algorithms allows together with “doctor+artificial intelligence” to improve the diagnosis of glaucoma.

• **KEYWORDS:** artificial intelligence; spectral-domain optical coherence tomography; glaucoma; Meta-analysis

**DOI:10.18240/ijo.2024.03.02**

**Citation:** Shi NN, Li J, Liu GH, Cao MF. Artificial intelligence for the detection of glaucoma with SD-OCT images: a systematic review and Meta-analysis. *Int J Ophthalmol* 2024;17(3):408-419

## INTRODUCTION

Glaucoma is a group of eye disorders characterized by chronically progressive disorders of the optic neuropathy<sup>[1]</sup>. It is the second most common cause of irreversible vision loss worldwide<sup>[2-3]</sup>. By 2040, the prevalence of glaucoma will increase to 111.8 million, resulting in a major public health problem that threatens national eye health<sup>[4]</sup>. It is classified into open angle glaucoma and angle-closure glaucoma according to the state of anterior chamber angle when intraocular pressure (IOP) increases. Primary open angle glaucoma (POAG), the most common form of glaucoma in western countries, is typically asymptomatic in its early stages and often diagnosed after irreversible visual damage has occurred<sup>[5]</sup>. Primary angle-closure glaucoma (PACG) which mostly occurred in east Asian countries is mainly an asymptomatic disease, in less than 1/3 of cases, patients appear with acute primary angle closure<sup>[3]</sup>. Due to the high incidence and risk, improving the efficiency of the early diagnosis of glaucoma is imperative.

Optical coherence tomography (OCT) is a common imaging technology in the evaluation of glaucomatous structural damage<sup>[6]</sup>. Recently, the spectral-domain OCT (SD-OCT) is rapidly advancing which can measure the retinal nerve fiber layer (RNFL) and ganglion cell-inner plexiform layer (GCIPL) with 3D image acquisition modes, repeatable registration and advanced segmentation algorithms<sup>[7]</sup>. SD-OCT which provides a higher axial resolution and a faster scan speed, has theoretical advantages in glaucoma assessment over the earlier generation of time domain (TD)-OCT<sup>[8-9]</sup>. Although glaucoma damage is irreversible, early diagnosis and treatment through

OCT images can prevent visual functional and structural loss. With the rapid development of computer and information technology, data information construction has been gradually integrated into every field of society. Therefore, how to use artificial intelligence (AI) to better serve massive data information in hospital management and optimize and guide disease diagnosis is attracting more and more attention in ophthalmology.

To date, the development of AI has an unstopped trend. AI is a branch of computer science that aims to create intelligent machines<sup>[10]</sup>. Machine learning (ML) is the use of data or previous experience to optimize the performance criteria of computer programs. Deep learning (DL) is a new research direction in ML. The motivation for DL research is to build neural networks that simulate the human brain for analysis and learning to interpret the data. AI technologies are becoming an alternative approach to conventional technologies. AI has been used in different medicine sectors, such as radiology<sup>[11]</sup>, pathology<sup>[12]</sup>, dermatology<sup>[13]</sup>, cardiology<sup>[14]</sup>, gastroenterology<sup>[15]</sup> and ophthalmology<sup>[10]</sup>. In the ophthalmology field, AI was applied in diabetic retinopathy, age-related macular degeneration, glaucoma, cataract, keratoconus, and so on from multimodality images including fundus photographs, OCT, fundus fluorescence angiography (FFA) and anterior segment photography<sup>[16]</sup>.

AI has fostered breakthroughs in the screening, diagnosis and detection of progression in the field of glaucoma<sup>[17]</sup>. There are four main approaches to screening patients for glaucoma: measuring IOP, examining the angle anatomy, evaluating the visual field (VF) and assessing optic nerve head (ONH) and nerve fiber layer (RNFL)<sup>[18-19]</sup>. Currently, AI is commonly used in glaucoma management including IOP, VF, false positive (FP), and OCT<sup>[20]</sup>. A prospective cross-sectional study demonstrated that automated IOP measurements using DL of Goldmann applanation tonometry (GAT) videos is comparable to standard GAT<sup>[21]</sup>. Another study merged VF and clinical data longitudinal datasets to assess the performance of ML, and their results showed that the model was able to extract spatio-temporal features other algorithms cannot, with better diagnostic capabilities [area under the receiver operating characteristic (AUROC): 0.89 to 0.93]<sup>[22]</sup>. Li *et al*<sup>[23]</sup> developed a clinical DL system for prediction and stratifying the risk of glaucoma onset and progression based on color FPs, the study results proved that the feasibility of DL algorithms in the early detection and prediction of glaucoma progression. AI, ML, and DL will play a crucial role in glaucoma, with implications for early diagnosis of vision impairment in the setting of aging populations globally<sup>[24]</sup>.

Together, AI is expected to provide automated devices to ophthalmologists for early diagnosis and timely treatment of

ocular disorders in the near future<sup>[25]</sup>. Therefore, we performed this systematic review and Meta-analysis to quantify the performance of AI for the detection of glaucoma in SD-OCT.

## MATERIALS AND METHODS

**Protocol and Registration** We registered our protocol on PROSPERO (<https://www.crd.york.ac.uk/PROSPERO/>), whose registration number was CRD42023431060. This systematic review and Meta-analysis adheres to The PRISMA extension for Diagnostic Test Accuracy (PRISMA-DTA) in 2018<sup>[26]</sup>.

**Eligibility Criteria** All papers that reported AI algorithms in SD-OCT images for glaucoma diagnosis were taken into account. The inclusion criteria in detail were as follows: 1) Based on AI including DL or ML, glaucoma can be detected by SD-OCT single-modal images or SD-OCT combined with VF/fundus photography multimodal images. 2) Clearing the definition of glaucoma including POAG or PACG or both. 3) The outcomes consist of sensitivity, specificity, and so on. 4) AI is generally divided into a test set and a training set, the training set is used to train the AI model for diagnosing glaucoma, and the test set ultimately selects the performance of the optimal model. Only the test set data were used for Meta-analysis in this study, and if the literature did not report the grouping of the specific training set and the test set, the data of the entire sample set were recorded. 5) The language is limited to English. The exclusion criteria were as follows: 1) ongoing or unpublished studies, 2) using other multimodality images such as fundus photographs, anterior segment-OCT and FFA, 3) publication forms including conference, review, Meta-analysis, and case report, 4) studies cannot extract the specific outcomes.

## Information Sources, Search Strategies and Study Selection

We searched six databases from PubMed, Web of Science, Cochrane Library, ScienceDirect, ProQuest and Scopus by May 31, 2023. The following search terms: “artificial intelligence”, “deep learning”, “machine learning”, “Computational Intelligence”, “Machine Intelligence”, “Computer Reasoning”, “Computer Vision System”, “Knowledge Acquisition”, “Knowledge Representation”, “glaucoma”, and “optical coherence tomography”.

**Data Collection and Definitions for Data Extraction** Two investigators (Shi NN, Li J) independently screened the literature, and if there were discrepancies in the results, the third investigator (Liu GH) would discuss them together. Then the data from the included studies were extracted by a researcher (Shi NN) and were rechecked by another (Cao MF). The extracted baseline data consist of study, year, study characteristics, datasets, device, total image numbers, image quality, outcome, method, methodology, sensitivity, and specificity.

**Risk of Bias and Applicability** Quality Assessment of Diagnostic Accuracy Studies-2 (QUADAS-2) has been widely used to assess the risk of bias in accuracy studies of diagnostic tests. QUADAS-2 tool is composed of patient selection, index test, reference standard, flow and timing. The first three parts are assessed in terms of clinical applicability. Two researchers (Shi NN, Li J) independently applied the QUADAS-2 tool to evaluate the quality of the included literature. If there were some disagreements, the third researcher (Liu GH) would negotiate and solve them.

**Diagnostic Accuracy Measures and Synthesis of Results**

The diagnostic accuracy indicators (sensitivity and specificity) of the included studies were reported in the baseline data table. The values of true positive (TP), FP, false negative (FN) and true negative (TN) were calculated by Review Manager5.4 according to the number of researchers, sensitivity, and specificity. For multiple groups of data in the same literature, we regarded each subgroup as an independent study in this meta-analysis. The sensitivity, specificity, positive likelihood ratio (PLR), negative likelihood ratio (NLR), diagnostic odds ratio (DOR), summary receiver operator characteristic (SROC) and area under curve (AUC) were combined to quantify the performance of AI for the detection of glaucoma in SD-OCT.

**Meta-analysis and Additional Analyses** The risk of bias for included studies was performed using Revman5.4. All Meta-analysis and addition analyses were presented with the Stata16.0. The Spearman correlation coefficient was first calculated to determine whether there was a threshold effect. When there was no threshold effect among the included studies, the Chi-square test was further used to analyze the statistical heterogeneity among the results of the included studies, and  $I^2$  was used to quantitatively determine the degree of heterogeneity. If  $I^2 < 50\%$ , the fixed effect model was applied for the combined analysis, otherwise the random effect model was used. Meta-regression was utilized to detect the cause of heterogeneity. Then, subgroup analyses were conducted according to different methods (regions, methods, outcomes, and devices). Deek’s funnel plot and sensitivity analysis were applied to judge the publication bias and evaluate the stability of the analysis results.

**RESULTS**

**Study Selection** We searched 1373 records initially, about 394 from PubMed, 324 from Web of Science, 17 from Cochrane Library, 79 from ScienceDirect, 275 from ProQuest, and 284 from Scopus. The 405 duplicates were removed, and then we excluded 903 by reading the titles and abstracts of the literature. Finally, the remaining 65 papers were downloaded in full text and screened carefully, resulting in the inclusion of 20 pieces of literature that met the eligible criteria. Figure 1 shows the literature selection process.

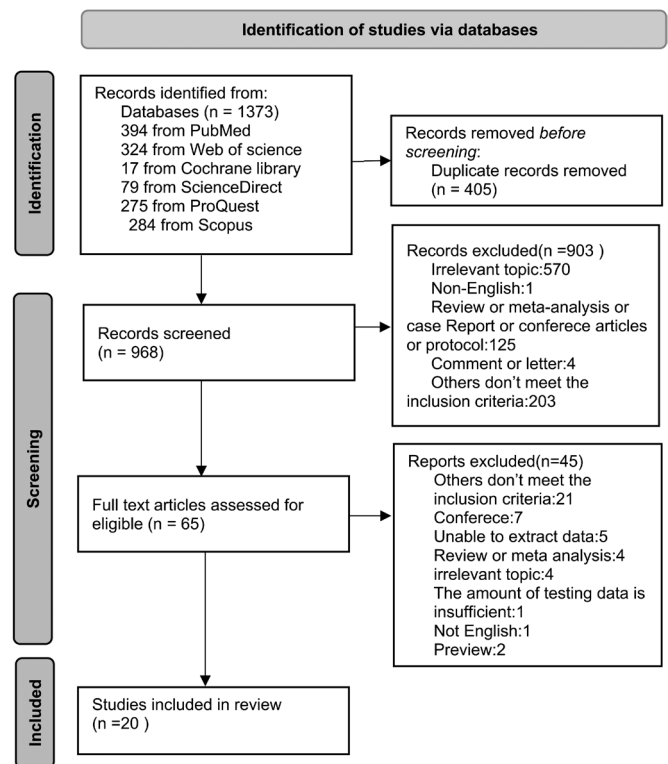


Figure 1 Study selection flow diagram.

**Study Characteristic** The detailed study characteristics are presented in Table 1. A total of 20 studies<sup>[27-46]</sup> were included in the article which comprises 51 models. The studies were published in years from 2014 to 2023 and involved 13 diverse countries/regions [Australia, Brazil, China, India, Japan, Korea, Pakistan, Singapore, Romania, Spain, Taiwan (China), United States, and Nepal], two of which were multicenter surveys. The types of research covered prospective, retrospective, cross-sectional, and cohort observational studies. In terms of the device, there were 3 types including Topcon 3D OCT, Heidelberg Spectralis OCT and Cirrus Zeiss OCT. Fourteen studies reported POAG as the outcome indicator, and the remaining covered glaucoma (POAG and PACG) as the outcome. The DL was a commonly used method and was adopted in 12 studies. The ML method was utilized in 7 studies. Only 1 article used both methods.

**Risk of Bias and Applicability** We applied the QUADAS-2 tool to assess the quality of included studies (Figure 2). The 13 included studies were high quality with low risk of bias and applicability concerns. There are 3 studies<sup>[27,30,41]</sup> that did not report whether consecutive or random cases were included, thus patient selection and applicability concerns were rated as “unclear risk”. Another 3 articles<sup>[39,43-44]</sup> could not judge whether the gold standard correctly distinguishes the target disease states, therefore we assess reference standard and applicability concerns as “unclear risk”. One study<sup>[43]</sup> was graded as “high risk” for flow and timing due to the modification of inclusion criteria after upgrading the software,

**Table 1 Basic characteristics of included studies**

Study	Country/region	Study characteristics	Datasets	Device	Modals	Total images	Image quality	Outcome	Method	Methodology	SEN/SPE
Zheng, 2020	China	Prospective observational study	Joint Shantou International Eye Center of Shantou University and the Chinese University of Hong Kong (JSIEC)	Topcon 3D OCT	OCT	1501	1024 points of resolution	Glaucoma	DL	CNN: Inception-V3	0.981/0.900
Yoshida, 2014	Japan	Prospective observational study	The University of Tokyo Hospital or the Tajimi Iwase Eye Clinic	Topcon 3D OCT	OCT	/	512x128 pixels	OAG	ML	RF	0.929/0.960
Wu, 2022	Taiwan, China	Cross-sectional study	The Fu-Jen Catholic University Hospital	Heidelberg Spectralis OCT	OCT	/	A quality index of at least 20	Glaucoma	ML	SVM	0.850/0.700
Wang, 2019	United States	Cohort study	The Los Angeles Latino Eye Study (LALES)	Cirrus 4000, ZEISS OCT	OCT	/	200x200 pixel	Glaucoma	ML	SVM KNN	0.817/0.960 0.828/0.883
Thompson, 2020	United States	Cross-sectional study	The Duke Glaucoma Repository	Heidelberg Spectralis OCT	OCT	20806	496x496 pixels	POAG	DL	ResNet-18 GlaucomaNet	0.860/0.838 0.828/0.914
Sun, 2021	Korea	Retrospective study	The Glaucoma Clinic, Seoul National University Hospital	Cirrus 6.0, ZEISS OCT	OCT	777	High-quality scans (signal strength $\geq 7$ )	POAG	DL	DICCN(RNFL/GCIPL) VGG16(RNFL) VGG16(GCIPL)	0.896/0.952 0.938/0.952 0.833/0.921
Singh, 2021	India	Retrospective study	Public (Mendeley) dataset and private dataset	/	OCT	/	200x200 dpi	OAG	ML	KNN SVM Decision Tree	1/0.857 0.800/0.660 1/0.750
Oh, 2021	Korea	Retrospective study	Gyeongsang National University Hospital	Heidelberg Spectralis OCT	OCT and VF	/	/	POAG or NTG	ML	RF LDA SVM	1/0.833 1/0.833 0.933/0.920
Noury, 2022	United States/China, India/Nepal	Multicenter retrospective study	Stanford School of Medicine, The Chinese University of Hong Kong, Narayana Nethralaya Foundation, and Tilganga Institute of Ophthalmology	Cirrus ZEISS OCT	OCT	2461	/	Glaucoma	Three-dimensional (3D) DL	C5.0 RF XGboost DiagFind	0.874/0.920 0.924/0.945 0.941/0.950 0.860/0.780 in US 0.730/0.730 in HK
Li, 2023	Singapore/Romania	Prospective cross-sectional study	The Singapore Eye Institute and the Department of Ophthalmology, Emergency University Hospital, Bucharest	Cirrus ZEISS OCT	OCT	/	/	POAG	ML	LR, SVM, RF and GB	0.930/0.710 in India 0.790/0.790 in Nepal 0.850/0.950 in Singapore 0.640/0.950 in Romania
Lee, 2020	Korea	Retrospective study	The Glaucoma Clinic, Seoul National University Hospital	Cirrus 6.0, ZEISS OCT	OCT	657	/	POAG	DL	NASNet	0.947/1
Kim, 2020	Korea	Retrospective study	The Glaucoma Clinic of Samsung Medical Center	Cirrus ZEISS OCT	OCT	7288	176x176 pixel	POAG	DL	CNN:VGG19	0.978/0.900

Table 1 Basic characteristics of included studies (continued)

Study	Country/region	Study characteristics	Datasets	Device	Modalities	Total images	Image quality	Outcome	Method	Methodology	SEN/SPE
García, 2021	Spain	Retrospective study	Institute for Research and Innovation in Bioengineering (I3B)	Heidelberg Spectralis OCT; Topcon 3D OCT	OCT	/	Cicr-DB-1/2: 496x768 pixels; void-DB-3: 885x512x128 voxels	POAG	DL	VGG16, VGG19, RAGNet with VGG16, RAGNet with VGG19	0.759/0.857
Escamez, 2021	Spain	Observational cross-sectional study	Fuenlabrada Hospital institution	Topcon 3D OCT	OCT	/	/	OAG	ML	The pruned decision tree	0.890/0.885
Barella, 2013	Brazil	Prospective, observational, cross-sectional study	The Glaucoma Service of the University of Campinas (UNICAMP)	Cirrus ZEISS OCT	OCT	/	/	POAG	ML	A modified tree	0.745/0.956
Asaoka, 2019	Japan	Prospective, multi-institution diagnosis study	The University of Tokyo Hospital, Inoue Eye Hospital, JR Tokyo General Hospital, Hiroshima Memorial Hospital, Osaka University Hospital, University Hospital of Kyoto Prefectural University of Medicine, and Oike Ikeda Eye Clinic	Topcon 3D OCT	OCT	4316	/	OAG	DL	/	0.578/0.800 0.684/0.800 0.450/0.800 0.560/0.800 0.491/0.800 0.719/0.800 0.649/0.800 0.614/0.800 0.460/0.800 0.736/0.800 0.866/0.900
Akter, 2022	Australia	Retrospective study	The Centre for Eye Health, UNSW Sydney	Cirrus ZEISS OCT; Heidelberg Spectralis OCT	OCT	/	383x197 pixels	POAG	DL	ResNet-18 VGG16	1/0.956 1/0.956
Song, 2022	China	Retrospective study	Zhongshan Ophthalmic Center (ZOC) OCT&VF	Topcon 3D OCT	OCT and VF	1395	good quality (without artifacts or blurs)	Glaucoma	DL	Proposed DL CNN	0.994/0.978 0.895/0.853
Raja, 2020	Pakistan	Retrospective study	Armed Forces Institute of Ophthalmology (AFIO): DATA1/DATA2	Topcon 3D OCT	OCT	196	951x456 pixels	Glaucoma	DL	CNN:VGG-16	0.979/0.870
Kim, 2017	Korea	Retrospective study	Dankook University Hospital and Gyeongsang National University Hospital	Heidelberg Spectralis OCT	OCT and VF	/	/	POAG or NTG	DL	C5.0 RF SVM KNN	0.983/0.950 0.983/0.975 0.983/0.950 0.967/0.975

SEN: Sensitivity; SPE: Specificity; DL: Deep learning; ML: Machine learning; CNN: Convolutional neural network; RF: Random forests; SVM: Support vector machine; KNN: K-Nearest Neighbor; ResNet: Residual deep convolutional neural network; DICNN: Dual-input convolutional neural network; RNFL: Retinal nerve fiber layer; GCPL: Ganglion cell-inner plexiform layer; LDA: Linear discriminant analysis; LR: Logistic regression; GB: Gradient boosting; NASNet: Neural architecture search network; RAGNet: Residual attention glaucoma network; BAG: Bagging; NB: Naive-bayes; SVM: Linear support vector machine; SVMG: Gaussian support vector machine; MLP: Multi\_x005f\_x005f\_x005f\_x0002\_layer\_perceptron; RBF: Radial basis function; RAN: Random forest; ENS: Ensemble selections; CTREE: Classification tree; ADA: AdaBoost M1; OAG: Open angle glaucoma; POAG: Primary open angle glaucoma; NTG: Normal tension glaucoma; OCT: Optical coherence tomography; VF: Visual field.



	Risk of Bias				Applicability Concerns		
	Patient Selection	Index Test	Reference Standard	Flow and Timing	Patient Selection	Index Test	Reference Standard
Akter2022	+	+	+	?	+	+	+
Asaoka2019	+	+	+	+	+	+	+
Barella2013	+	+	?	-	+	+	?
Escamez2021	+	+	?	+	+	+	?
Garcia2021	+	+	+	+	+	+	+
Kim2017	+	+	+	+	+	+	+
Kim2020	+	+	+	+	+	+	+
Lee2020	+	+	+	+	+	+	+
Li2023	+	+	+	+	+	+	+
Noury2022	+	+	+	+	+	+	+
Oh2021	+	+	+	+	+	+	+
Raja2020	+	+	?	+	+	+	?
Singh2021	?	+	+	+	?	+	+
Song2022	?	+	+	+	?	+	+
Sun2021	+	+	+	+	+	+	+
Thompson2020	+	+	+	+	+	+	+
Wang2019	+	+	+	+	+	+	+
Wu2022	?	+	+	+	?	+	+
Yoshida2014	+	+	+	+	+	+	+
Zheng2020	+	+	+	+	+	+	+

● High
? Unclear
+ Low

Figure 2 Risk of bias assessment of included studies via QUADAS-2 tool.

which resulted in not all participants being enrolled in the analysis. The other study<sup>[42]</sup> extracted possible diagnostic features of glaucoma and did not indicate whether all patients received only the same gold standard, so flow and timing was given an “unclear risk”.

**Performance of AI in Glaucoma Detection and Synthesis of Results** The threshold analysis was tested first whether there was a threshold effect. The result proved there was a low heterogeneity (Spearman correlation coefficient =0.22). Figure 3 demonstrates the paired forest plot for sensitivity and specificity with 95% CIs for each study. The pooled sensitivity and specificity were 0.91 (95%CI: 0.86–0.94,  $I^2=94.67%$ ), 0.90 (95%CI: 0.87–0.92,  $I^2=89.24%$ ). Figure 4 displays the paired forest plot for PLR and NLR with 95% CIs for each study. The pooled PLR and NLR were 8.79 (95%CI: 6.93–11.15,  $I^2=89.31%$ ), 0.11 (95%CI: 0.07–0.16,  $I^2=95.25%$ ). Figure 5 shows the forest plot for DOR and SROC curve with 95% CIs. The pooled DOR and AUC were 83.58 (95%CI: 47.15–148.15,  $I^2=100%$ ), 0.95 (95%CI: 0.93–0.97).

**Addition Analyses** With the high heterogeneity of this Meta-analysis, Meta-regression was performed to analyze the reasons. We proceeded with the analysis in four dimensions, namely, regions, methods, outcomes, and devices. Then, subgroup analyses were conducted according to diverse causes. The detailed results showed in Table 2. Deek’s funnel plot of each mode 1 (Figure 6) was tested to evaluate the publication bias ( $P=0.32$ ), which indicated no clear bias in this Meta-analysis. The result of sensitivity analysis was presented in Figure 7. The picture clearly showed that the Meta-analysis has good stability.

**DISCUSSION**

The diagnosis of glaucoma in its early stages is challenging. This Meta-analysis included 20 studies and 51 models in order to investigate the performance of AI in detecting glaucoma. Based on our results of Meta-analysis in the paper, it is confirmed that there is a high accuracy for the detection of glaucoma with AI in SD-OCT images. Thus, the application of AI-based tools for detecting glaucoma may provide substantial benefits for early detection, prevention, and treatment of the disease.

Glaucoma is an eye disease that causes optic nerve damage and progressive VF loss due to increased IOP<sup>[47]</sup>. This leads to progressive deterioration of the VF, usually starting from the mid-periphery and progressing in a centripetal direction until eventually only a central or peripheral vision remains<sup>[48]</sup>. The early stage of glaucoma is not easy to be detected, resulting in delayed treatment and irreversible visual impairment. Therefore, early detection is essential to glaucoma treatment as it can prevent further vision loss<sup>[3]</sup>.

Common to all glaucomatous eyes is the loss of retinal ganglion cells and thinning of the RNFL, particularly the cup thinning of the optic disc<sup>[49]</sup>. Rapid advances in ophthalmic imaging in recent years have presented opportunities and challenges. Assessment of the optic disc and VF using OCT imaging, fundus photography, and standard automated VF meter helps in the clinical diagnosis of optic nerve damage in glaucoma<sup>[50]</sup>. Detection of structural changes in glaucoma has traditionally relied on the evaluation of fundus photographs. However, photographs cannot be quantified and there is little consistency in experts’ judgment of optic disc photographs. OCT overcomes the limitations of fundus photography by allowing objective quantitative measurements of the RNFL, optic disc, and macula, which can aid in the diagnosis and progression analysis of glaucoma<sup>[51]</sup>. In contrast to OCT, the ability of VF examinations to detect disease progression is influenced by the stage of the disease. In the natural course of glaucoma, structural and functional damage may not occur at the same time, and in the early stages, the likelihood of detecting disease using OCT is higher because structural

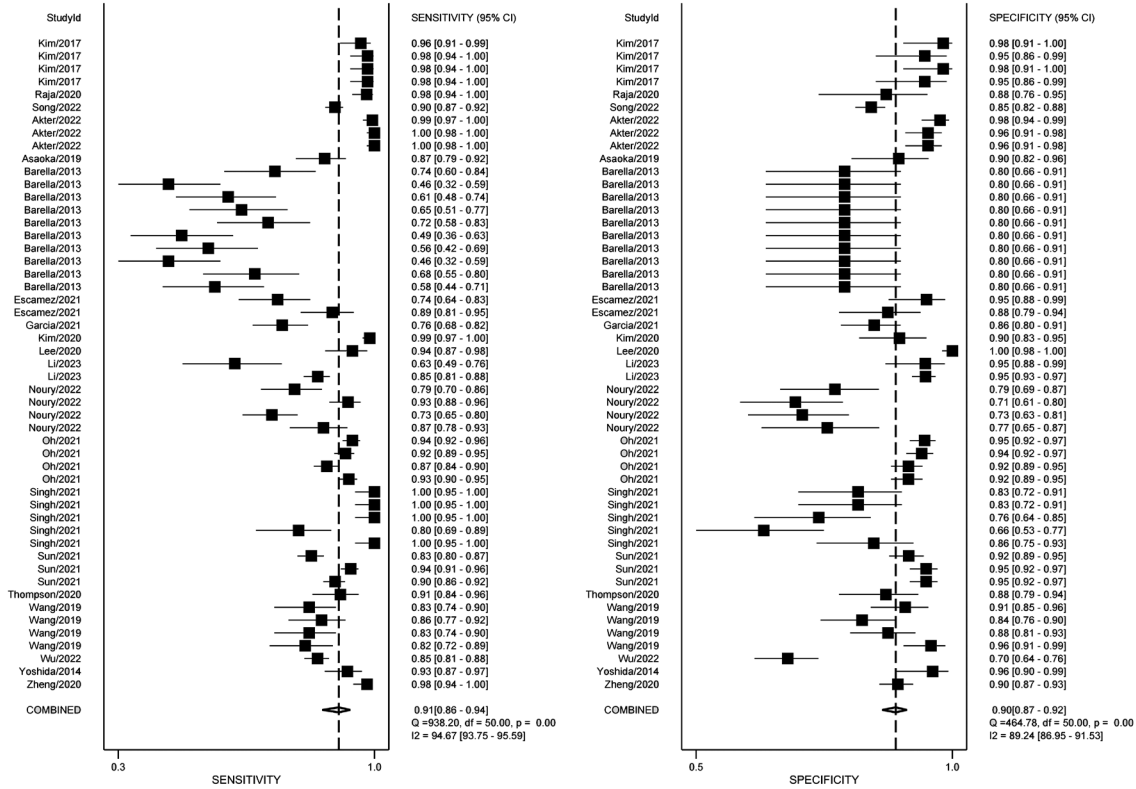


Figure 3 The forest plot of the pooled sensitivity and specificity.

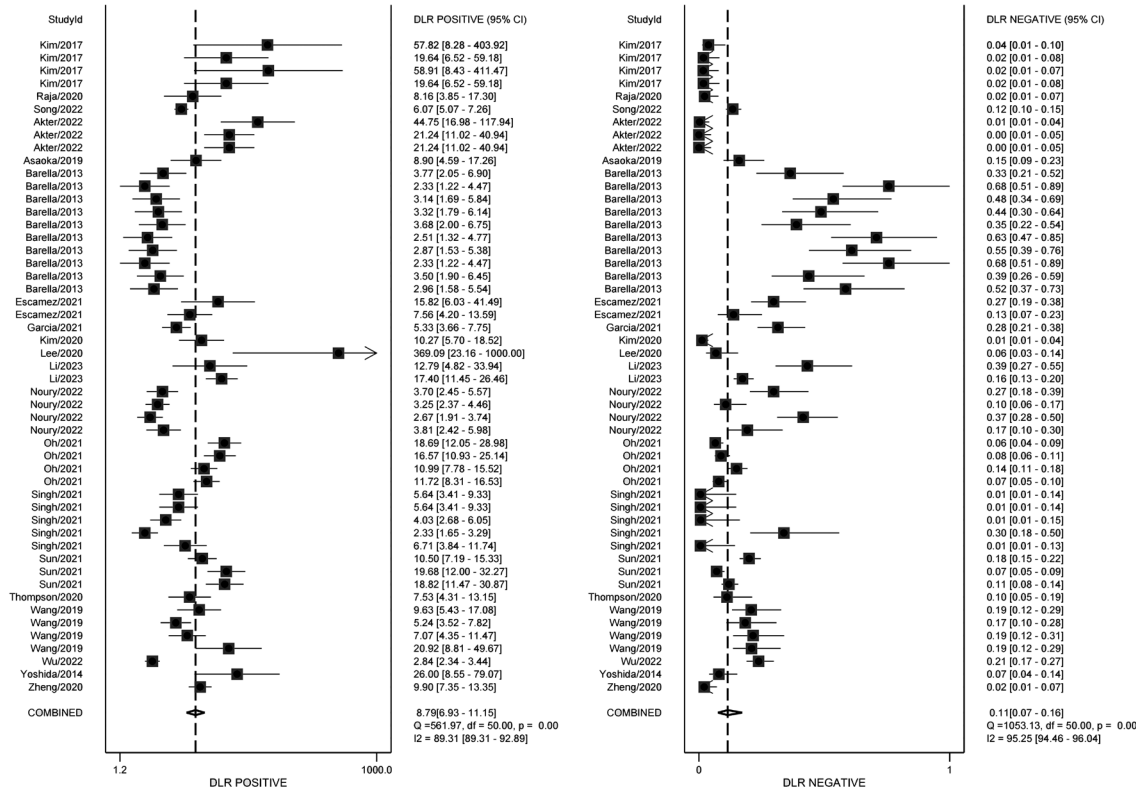


Figure 4 The forest plot of the PLR and NLR PLR: Positive likelihood ratio; NLR: Negative likelihood ratio.

changes such as ganglion cell loss and thinning of the RNFL usually occur before loss of function as detected by conventional VF testing<sup>[52]</sup>. In advanced stages of the disease, loss of function and thus VF defects are more appropriate to be detected using VF testing<sup>[53-54]</sup>. Reliable computer-assisted

diagnosis of glaucoma has continued to expand in recent years. One is the single-path method, which inputs single-type data. The other is a multimodal fusion image, which is combined with two or more types of data<sup>[55]</sup>. A number of studies have shown that multimodal imaging based on DL can detect

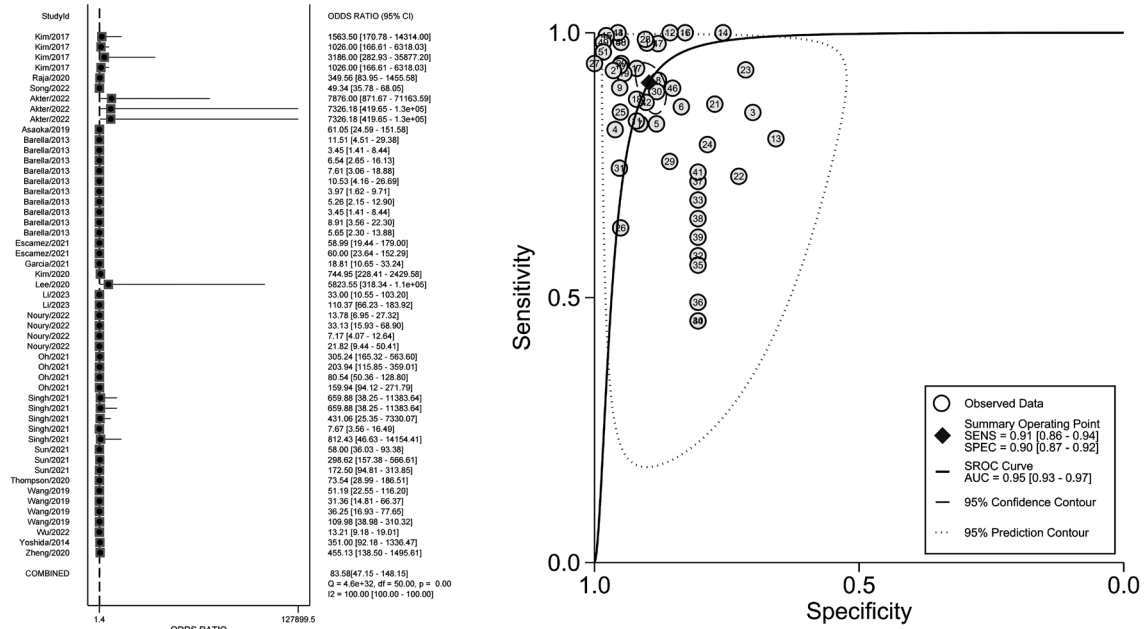


Figure 5 The forest plot of the DOR and SROC curve DOR: Diagnostic odds ratio; SROC: Summary receiver operator characteristic.

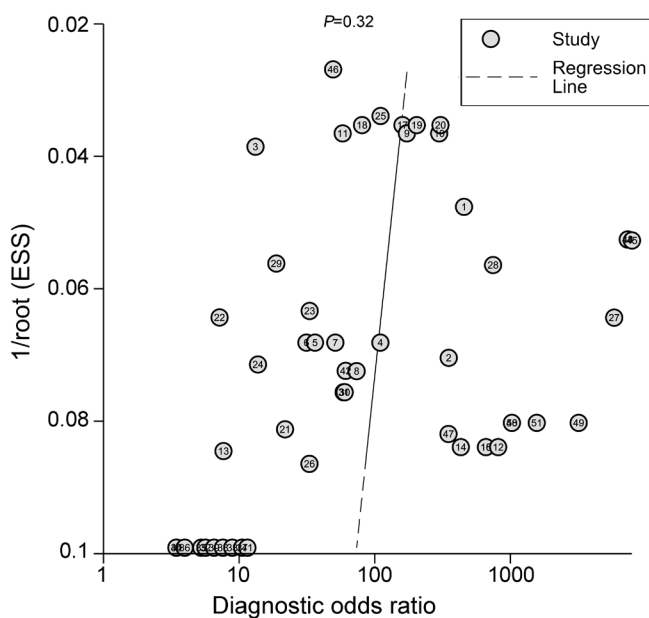


Figure 6 Deek's funnel plot of each model.

glaucoma with higher accuracy, which can further improve the performance of glaucoma diagnosis<sup>[55-57]</sup>. OCT is a non-invasive imaging technique<sup>[58]</sup>. In recent years, there has been a continuous iteration of OCT technology, from the earliest TD-OCT to the current SD-OCT and swept-source OCT (SS-OCT). The latter achieves faster scanning and higher axial resolution and incorporates innovations such as real-time eye-tracking to compensate for eye movements during data acquisition and minimize motion artifacts<sup>[59]</sup>. SD-OCT is currently one of the most commonly used auxiliary tests for the diagnosis of glaucoma<sup>[60]</sup>. However, the diagnostic accuracy may be challenged by the enormous workload due to the necessity of manual image processing, relevant inter-

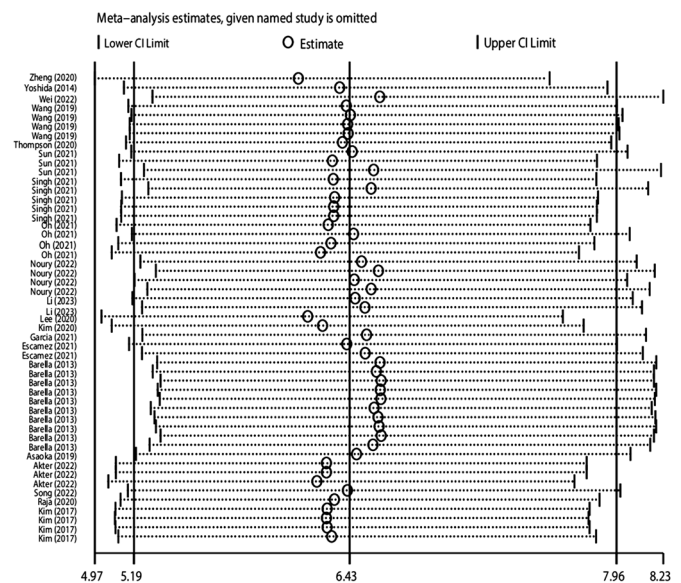


Figure 7 Sensitivity analysis of each model.

observer variability, and interference factors (e.g., extreme refractive errors). Currently, AI is generating global interest. The development of AI algorithms to analyze images and reach the diagnosis of diseases has a huge impact on the medical field<sup>[61]</sup>. Hence, improving the diagnostic efficacy of glaucoma based on AI algorithms combined with SD-OCT images can help ophthalmologists make quick clinical decisions and further facilitate glaucoma screening. As shown in Figures 3–5, our results yielded robust and consistent findings that lend support to the high diagnostic accuracy of AI for the detection of glaucoma in SD-OCT images. In this Meta-analysis, there exists a high accuracy in detecting glaucoma, but with high heterogeneity. We performed Meta-regression, with heterogeneity originating



Table 2 Subgroup analyses and Meta-regression results

Variables	No. of models	Sensitivity		Specificity		PLR		NLR		DOR		Meta regression	
		Pooled (95%CI)	I <sup>2</sup>	Pooled (95%CI)	I <sup>2</sup>	Pooled (95%CI)	I <sup>2</sup>	Pooled (95%CI)	I <sup>2</sup>	Pooled (95%CI)	I <sup>2</sup>	AUC	P
Region													
Asian	28	0.94 (0.92, 0.96)	92.62%	0.91 (0.87, 0.94)	94.06%	10.39 (7.38, 14.63)	93.74%	0.06 (0.04, 0.09)	93.52%	168.82 (90.82, 313.80)	100%	0.97	0.00
Western	23	0.82 (0.70, 0.89)	93.54%	0.88 (0.85, 0.91)	75.45%	6.84 (4.81, 9.70)	76.38%	0.21 (0.12, 0.36)	92.69%	33.08 (13.85, 79.05)	100%	0.92	0.00
Method													
ML	27	0.84 (0.76, 0.90)	94.23%	0.87 (0.84, 0.90)	88.56%	6.67 (5.05, 8.79)	87.11%	0.18 (0.11, 0.29)	94.54%	36.98 (19.30, 70.86)	100%	0.92	0.06
DL	24	0.95 (0.91, 0.97)	94.71%	0.92 (0.89, 0.94)	92.60%	11.94 (8.23, 17.32)	92.05%	0.06 (0.03, 0.10)	95.12%	209.55 (91.56, 4779.59)	100%	0.98	
Outcome													
OAG	39	0.91 (0.86, 0.95)	95.38%	0.91 (0.89, 0.93)	85.87%	10.23 (7.73, 13.55)	86.58%	0.10 (0.06, 0.16)	95.89%	107.50 (52.10, 221.80)	100%	0.96	
Glaucoma	12	0.88 (0.83, 0.92)	88.39%	0.84 (0.79, 0.89)	88.18%	5.62 (4.09, 7.74)	85.38%	0.14 (0.09, 0.21)	89.44%	40.55 (21.54, 76.32)	100%	0.93	
Device													
Topcon 3D OCT	7	0.92 (0.85, 0.96)	89.58%	0.90 (0.87, 0.93)	71.39%	9.59 (6.89, 13.36)	50.19%	0.09 (0.05, 0.17)	89.10%	108.97 (52.58, 225.86)	100%	0.95	0.58
Heidelberg Spectralis OCT	10	0.94 (0.91, 0.96)	93.56%	0.94 (0.89, 0.97)	96.22%	15.72 (8.66, 28.53)	95.81%	0.06 (0.04, 0.10)	95.06%	243.19 (91.31, 647.67)	100%	0.98	0.02
Cirrus ZEISS OCT	30	0.85 (0.77, 0.90)	93.78%	0.87 (0.83, 0.90)	86.96%	6.38 (4.78, 8.52)	83.98%	0.17 (0.11, 0.27)	93.84%	36.70 (19.21, 70.13)	100%	0.92	0.00

DL: Deep learning; ML: Machine learning; OAG: Open angle glaucoma; PLR: Positive likelihood ratio; NLR: Negative likelihood ratio; DOR: Diagnostic odds ratio; AUC: Area under curve.

from regions, methods, outcomes and devices. Results indicate better diagnostic efficacy in detecting glaucoma in Asia than in Western countries. It may be related to the high prevalence of glaucoma in Asia<sup>[4]</sup>. In recent years, genetic and genomic studies have identified important genes associated with glaucoma that influence biological pathways and processes<sup>[62]</sup>. In the future, the genetic architecture of glaucoma can be determined in one step, enabling comprehensive genetic testing and gene-targeted therapy<sup>[63]</sup>. In traditional forms, ML still requires human-designed code to convert raw data into input features<sup>[64]</sup>. DL is a class of state-of-the-art ML techniques. DL models are a type of artificial neural network composed of several layers of artificial “neurons”<sup>[65]</sup>. It is confirmed in several studies that DL systems have great potential to improve glaucoma diagnosis<sup>[66-68]</sup>. While DL programs are not standardized, and they generate great dependence on the clinician on their final provider and cost. SD-OCT, which could measure the ONH, RNFL, and macular parameters has been a vital image modality in glaucoma practice<sup>[69]</sup>. *Pierro et al*<sup>[70]</sup> evaluated the RNFL reproducibility of various SD-OCTs and showed that Heidelberg demonstrated high inter-operator agreement. However, digital imaging in glaucoma continues to develop, different devices perform high diagnostic capabilities and are complementary to each other<sup>[71]</sup>. This paper reviews different studies from around the world demonstrating the ability of AI algorithms to diagnose glaucoma using OCT images. As ophthalmic imaging technology continues to evolve, AI may play an important role in the near future of healthcare<sup>[72]</sup>. The main shortcoming of this Meta-analysis is that the datasets are different and the algorithms used in each study are their own algorithms. Besides, a limitation of this analysis is that the diagnosis of glaucoma was not the result of a single test but rather an integrated interpretation of risk factors. Therefore, misclassification due to this subjective assessment cannot be completely ruled out. Future observations will be needed to see how AI algorithms, when integrated with clinical practice, affect clinical diagnosis and assess changes over time. Third, many glaucoma patients have cataracts and corneal opacities, which reduce the quality of the images. The performance of DL and ML algorithms depends on the quality of the images, and the exclusion of low-quality images from the study may limit the effectiveness of the algorithms in real clinical applications. Fourth, since the structural data were trained and validated by the DL classifier, this might have biased the diagnostic ability by overestimating the sensitivity-specificity balance. It is also the reason of the high number of works with sensitivity/specificity closed to 1. Fifth, the Meta-analysis in this paper did not incorporate the training set. In the future, it is necessary to increase the size of the dataset to validate the AI

algorithm and improve its diagnostic accuracy for glaucoma. Sixth, we did not compare the performance between AI and human experts since limited data were available. Seventh, due to the widespread use of SD-OCT, only studies with SD-OCT were included in this study. However, with the continuous development of ophthalmic imaging technology, it is necessary to expand the scope of research to swept-source OCT in the future. Additionally, some of included studies were reported without specification. We should enhance the quality and reliability of clinical ophthalmic AI research by following the guidelines<sup>[73]</sup>. Finally, many AI programs work on the black box, the internal algorithm-specific features extracted by DL are especially complex to understand. It is imperative to develop explainable AI (XAI) so as to interpret trained deep networks to unbox the black-box<sup>[74]</sup>.

In conclusion, our study found that AI is promising in detecting glaucoma from SD-OCT. The application of AI-based algorithms allows together with “doctor+artificial intelligence” to improve the diagnosis of glaucoma. Improving the diagnostic efficacy of glaucoma based on AI algorithms combined with SD-OCT images can help ophthalmologists make quick clinical decisions and further facilitate glaucoma screening. More datasets established by new diagnostic methods will be used in the future, which will be helpful in fundus application screening, and reducing the work-load of physicians.

#### ACKNOWLEDGEMENTS

**Conflicts of Interest:** Shi NN, None; Li J, None; Liu GH, None; Cao MF, None.

#### REFERENCES

- Schuster AK, Erb C, Hoffmann EM, Dietlein T, Pfeiffer N. The diagnosis and treatment of glaucoma. *Dtsch Arztebl Int* 2020;117(13):225-234.
- Quigley HA, Broman AT. The number of people with glaucoma worldwide in 2010 and 2020. *Br J Ophthalmol* 2006;90(3):262-267.
- Weinreb RN, Aung T, Medeiros FA. The pathophysiology and treatment of glaucoma: a review. *JAMA* 2014;311(18):1901-1911.
- Tham YC, Li X, Wong TY, Quigley HA, Aung T, Cheng CY. Global prevalence of glaucoma and projections of glaucoma burden through 2040: a systematic review and meta-analysis. *Ophthalmology* 2014;121(11):2081-2090.
- Weinreb RN, Khaw PT. Primary open-angle glaucoma. *Lancet* 2004;363(9422):1711-1720.
- Inoue R, Hangai M, Kotera Y, Nakanishi H, Mori S, Morishita S, Yoshimura N. Three-dimensional high-speed optical coherence tomography imaging of lamina cribrosa in glaucoma. *Ophthalmology* 2009;116(2):214-222.
- Bussell II, Wollstein G, Schuman JS. OCT for glaucoma diagnosis, screening and detection of glaucoma progression. *Br J Ophthalmol* 2014;98(Suppl 2):ii15-ii19.
- Sung KR, Kim DY, Park SB, Kook MS. Comparison of retinal nerve fiber layer thickness measured by cirrus HD and stratus optical coherence tomography. *Ophthalmology* 2009;116(7):1264-1270.e1.
- Leung CK, Cheung CY, Weinreb RN, et al. Retinal nerve fiber layer imaging with spectral-domain optical coherence tomography: a variability and diagnostic performance study. *Ophthalmology* 2009;116(7):1257-1263, 1263.e1-1263.e2.
- Schmidt-Erfurth U, Sadeghipour A, Gerendas BS, Waldstein SM, Bogunović H. Artificial intelligence in retina. *Prog Retin Eye Res* 2018;67:1-29.
- Hosny A, Parmar C, Quackenbush J, Schwartz LH, Aerts HJWL. Artificial intelligence in radiology. *Nat Rev Cancer* 2018;18(8):500-510.
- Bi WL, Hosny A, Schabath MB, et al. Artificial intelligence in cancer imaging: clinical challenges and applications. *CA Cancer J Clin* 2019;69(2):127-157.
- Du-Harpur X, Watt FM, Luscombe NM, Lynch MD. What is AI? Applications of artificial intelligence to dermatology. *Br J Dermatol* 2020;183(3):423-430.
- Johnson KW, Torres Soto J, Glicksberg BS, Shameer K, Miotto R, Ali M, Ashley E, Dudley JT. Artificial intelligence in cardiology. *J Am Coll Cardiol* 2018;71(23):2668-2679.
- Le Berre C, Sandborn WJ, Aridhi S, Devignes MD, Fournier L, Smail-Tabbone M, Danese S, Peyrin-Biroulet L. Application of artificial intelligence to gastroenterology and hepatology. *Gastroenterology* 2020;158(1):76-94.e2.
- Moraru AD, Costin D, Moraru RL, Branisteanu DC. Artificial intelligence and deep learning in ophthalmology - present and future (Review). *Exp Ther Med* 2020;20(4):3469-3473.
- Li JO, Liu HR, Ting DSJ, et al. Digital technology, tele-medicine and artificial intelligence in ophthalmology: a global perspective. *Prog Retin Eye Res* 2021;82:100900.
- Prum BE Jr, Herndon LW Jr, Moroi SE, et al. Primary angle closure preferred practice pattern<sup>®</sup> guidelines. *Ophthalmology* 2016;123(1):P1-P40.
- Prum BE, Rosenberg LF, Gedde SJ, et al. Primary open-angle glaucoma preferred practice pattern<sup>®</sup> guidelines. *Ophthalmology* 2016;123(1):P41-P111.
- Zhang LY, Tang L, Xia M, Cao GF. The application of artificial intelligence in glaucoma diagnosis and prediction. *Front Cell Dev Biol* 2023;11:1173094.
- Spaide T, Wu Y, Yanagihara RT, et al. Using deep learning to automate goldmann applanation tonometry readings. *Ophthalmology* 2020;127(11):1498-1506.
- Dixit A, Yohannan J, Boland MV. Assessing glaucoma progression using machine learning trained on longitudinal visual field and clinical data. *Ophthalmology* 2021;128(7):1016-1026.
- Li F, Su YD, Lin FB, et al. A deep-learning system predicts glaucoma incidence and progression using retinal photographs. *J Clin Invest* 2022;132(11):e157968.
- Ting DSJ, Peng L, Varadarajan AV, et al. Deep learning in ophthalmology: the technical and clinical considerations. *Prog Retin Eye Res* 2019;72:100759.

- 25 Balyen L, Peto T. Promising artificial intelligence-machine learning-deep learning algorithms in ophthalmology. *Asia Pac J Ophthalmol* 2019;8(3):264-272.
- 26 McInnes MDF, Moher D, Thombs BD, *et al.* Preferred reporting items for a systematic review and meta-analysis of diagnostic test accuracy studies: the PRISMA-DTA statement. *JAMA* 2018;319(4):388-396.
- 27 Singh LK, Pooja, Garg H, Khanna M. An artificial intelligence-based smart system for early glaucoma recognition using OCT images. *Int J E Health Med Commun* 2021;12(4):32-59.
- 28 Li C, Chua J, Schwarzhans F, *et al.* Assessing the external validity of machine learning-based detection of glaucoma. *Sci Rep* 2023;13(1):558.
- 29 Thompson AC, Jammal AA, Berchuck SI, Mariottoni EB, Medeiros FA. Assessment of a segmentation-free deep learning algorithm for diagnosing glaucoma from optical coherence tomography scans. *JAMA Ophthalmol* 2020;138(4):333-339.
- 30 Song DP, Li F, Li C, Xiong J, He JJ, Zhang XL, Qiao Y. Asynchronous feature regularization and cross-modal distillation for OCT based glaucoma diagnosis. *Comput Biol Med* 2022;151(Pt B):106283.
- 31 Noury E, Mannil SS, Chang RT, *et al.* Deep learning for glaucoma detection and identification of novel diagnostic areas in diverse real-world datasets. *Transl Vis Sci Technol* 2022;11(5):11.
- 32 Zheng C, Xie XL, Huang LT, *et al.* Detecting glaucoma based on spectral domain optical coherence tomography imaging of peripapillary retinal nerve fiber layer: a comparison study between hand-crafted features and deep learning model. *Graefes Arch Clin Exp Ophthalmol* 2020;258(3):577-585.
- 33 Kim KE, Kim JM, Song JE, Kee C, Han JC, Hyun SH. Development and validation of a deep learning system for diagnosing glaucoma using optical coherence tomography. *J Clin Med* 2020;9(7):2167.
- 34 Kim SJ, Cho KJ, Oh S. Development of machine learning models for diagnosis of glaucoma. *PLoS One* 2017;12(5):e0177726.
- 35 Lee J, Kim YK, Park KH, Jeoung JW. Diagnosing glaucoma with spectral-domain optical coherence tomography using deep learning classifier. *J Glaucoma* 2020;29(4):287-294.
- 36 Yoshida T, Iwase A, Hirasawa H, Murata H, Mayama C, Araie M, Asaoka R. Discriminating between glaucoma and normal eyes using optical coherence tomography and the 'Random Forests' classifier. *PLoS One* 2014;9(8):e106117.
- 37 Sun S, Ha A, Kim YK, Yoo BW, Kim HC, Park KH. Dual-input convolutional neural network for glaucoma diagnosis using spectral-domain optical coherence tomography. *Br J Ophthalmol* 2021;105(11):1555-1560.
- 38 Oh S, Park Y, Cho KJ, Kim SJ. Explainable machine learning model for glaucoma diagnosis and its interpretation. *Diagnostics* 2021;11(3):510.
- 39 Raja H, Akram MU, Shaukat A, Khan SA, Alghamdi N, Khawaja SG, Nazir N. Extraction of retinal layers through convolution neural network (CNN) in an OCT image for glaucoma diagnosis. *J Digit Imaging* 2020;33(6):1428-1442.
- 40 García G, Colomer A, Naranjo V. Glaucoma detection from raw SD-OCT volumes: a novel approach focused on spatial dependencies. *Comput Methods Programs Biomed* 2021;200:105855.
- 41 Wu CW, Chen HY, Chen JY, Lee CH. Glaucoma detection using support vector machine method based on spectralis OCT. *Diagnostics* 2022;12(2):391.
- 42 Akter N, Fletcher J, Perry S, Simunovic MP, Briggs N, Roy M. Glaucoma diagnosis using multi-feature analysis and a deep learning technique. *Sci Rep* 2022;12(1):8064.
- 43 Barella KA, Costa VP, Gonçalves Vidotti V, Silva FR, Dias M, Gomi ES. Glaucoma diagnostic accuracy of machine learning classifiers using retinal nerve fiber layer and optic nerve data from SD-OCT. *J Ophthalmol* 2013;2013:789129.
- 44 Escamez CSF, Martinez SP, Fernandez NT. High interpretable machine learning classifier for early glaucoma diagnosis. *Int J Ophthalmol* 2021;14(3):393-398.
- 45 Wang PY, Shen J, Chang R, *et al.* Machine learning models for diagnosing glaucoma from retinal nerve fiber layer thickness maps. *Ophthalmol Glaucoma* 2019;2(6):422-428.
- 46 Asaoka R, Murata H, Hirasawa K, *et al.* Using deep learning and transfer learning to accurately diagnose early-onset glaucoma from macular optical coherence tomography images. *Am J Ophthalmol* 2019;198:136-145.
- 47 Michels TC, Ivan O. Glaucoma: diagnosis and management. *Am Fam Physician* 2023;107(3):253-262.
- 48 Quigley HA. Glaucoma. *Lancet* 2011;377(9774):1367-1377.
- 49 Lee JWY, Chan PP, Zhang XJ, Chen LJ, Jonas JB. Latest developments in normal-pressure glaucoma: diagnosis, epidemiology, genetics, etiology, causes and mechanisms to management. *Asia Pac J Ophthalmol* 2019;8(6):457-468.
- 50 Mursch-Edlmayr AS, Ng WS, Diniz-Filho A, *et al.* Artificial intelligence algorithms to diagnose glaucoma and detect glaucoma progression: translation to clinical practice. *Transl Vis Sci Technol* 2020;9(2):55.
- 51 Tatham AJ, Medeiros FA. Detecting structural progression in glaucoma with optical coherence tomography. *Ophthalmology* 2017;124(12S):S57-S65.
- 52 Kang JM, Tanna AP. Glaucoma. *Med Clin N Am* 2021;105(3):493-510.
- 53 Shigueoka LS, Vasconcellos JPC, Schimiti RB, *et al.* Automated algorithms combining structure and function outperform general ophthalmologists in diagnosing glaucoma. *PLoS One* 2018;13(12):e0207784.
- 54 Harwerth RS, Wheat JL, Fredette MJ, Anderson DR. Linking structure and function in glaucoma. *Prog Retin Eye Res* 2010;29(4):249-271.
- 55 Yi SL, Zhang G, Qian CX, Lu YQ, Zhong H, He JF. A multimodal classification architecture for the severity diagnosis of glaucoma based on deep learning. *Front Neurosci* 2022;16:939472.
- 56 Huang XQ, Sun J, Gupta K, *et al.* Detecting glaucoma from multi-modal data using probabilistic deep learning. *Front Med* 2022;9:923096.

- 57 Xiong J, Li F, Song DP, *et al.* Multimodal machine learning using visual fields and peripapillary circular OCT scans in detection of glaucomatous optic neuropathy. *Ophthalmology* 2022;129(2):171-180.
- 58 Wu CW, Shen HL, Lu CJ, Chen SH, Chen HY. Comparison of different machine learning classifiers for glaucoma diagnosis based on spectralis OCT. *Diagnostics* 2021;11(9):1718.
- 59 Kim MS, Nam KY, Hwang YH, Lee MW, Lee WH, Lim HB, Kim JY. Effect of Weiss ring on peripapillary retinal nerve fiber layer thickness measurements using SD-OCT. *Sci Rep* 2022;12(1):17357.
- 60 Renard JP, Fénolland JR, Giraud JM. Glaucoma progression analysis by Spectral-Domain Optical Coherence Tomography (SD-OCT). *J Fr Ophtalmol* 2019;42(5):499-516.
- 61 Tabuchi H. Understanding required to consider AI applications to the field of ophthalmology. *Taiwan J Ophthalmol* 2022;12(2):123-129.
- 62 Wiggs JL, Pasquale LR. Genetics of glaucoma. *Hum Mol Genet* 2017;26(R1):R21-R27.
- 63 Wang ZX, Wiggs JL, Aung T, Khawaja AP, Khor CC. The genetic basis for adult onset glaucoma: recent advances and future directions. *Prog Retin Eye Res* 2022;90:101066.
- 64 Thompson AC, Jammal AA, Medeiros FA. A review of deep learning for screening, diagnosis, and detection of glaucoma progression. *Transl Vis Sci Technol* 2020;9(2):42.
- 65 Ting DSW, Pasquale LR, Peng L, *et al.* Artificial intelligence and deep learning in ophthalmology. *Br J Ophthalmol* 2019;103(2):167-175.
- 66 Hood DC, La Bruna S, Tsamis E, *et al.* Detecting glaucoma with only OCT: implications for the clinic, research, screening, and AI development. *Prog Retin Eye Res* 2022;90:101052.
- 67 Nakahara K, Asaoka R, Tanito M, *et al.* Deep learning-assisted (automatic) diagnosis of glaucoma using a smartphone. *Br J Ophthalmol* 2022;106(4): 587-592.
- 68 Kashyap R, Nair R, Gangadharan SMP, Botto-Tobar M, Farooq S, Rizwan A. Glaucoma detection and classification using improved U-net deep learning model. *Healthcare* 2022;10(12):2497.
- 69 Vazquez LE, Bye A, Aref AA. Recent developments in the use of optical coherence tomography for glaucoma. *Curr Opin Ophthalmol* 2021;32(2):98-104.
- 70 Pierro L, Gagliardi M, Iuliano L, Ambrosi A, Bandello F. Retinal nerve fiber layer thickness reproducibility using seven different OCT instruments. *Invest Ophthalmol Vis Sci* 2012;53(9):5912-5920.
- 71 Huang JJ, Liu X, Wu ZQ, Guo XX, Xu HZ, Dustin L, Sadda S. Macular and retinal nerve fiber layer thickness measurements in normal eyes with the Stratus OCT, the Cirrus HD-OCT, and the Topcon 3D OCT-1000. *J Glaucoma* 2011;20(2):118-125.
- 72 Kapoor R, Whigham BT, Al-Aswad LA. Artificial intelligence and optical coherence tomography imaging. *Asia Pac J Ophthalmol* 2019;8(2):187-194.
- 73 Yang WH, Shao Y, Xu YW, Expert Workgroup of Guidelines on Clinical Research Evaluation of Artificial Intelligence in Ophthalmology (2023), Ophthalmic Imaging and Intelligent Medicine Branch of Chinese Medicine Education Association Intelligent Medicine Committee of Chinese Medicine Education Association. Guidelines on clinical research evaluation of artificial intelligence in ophthalmology (2023). *Int J Ophthalmol* 2023;16(9):1361-1372.
- 74 Hasan MM, Phu J, Sowmya A, Meijering E, Kalloniatis M. Artificial intelligence in the diagnosis of glaucoma and neurodegenerative diseases. *Clin Exp Optom* 2023:1-17.